World Academy of Science, Engineering and Technology
International Journal of Energy and Power Engineering
Vol:10, No:1, 2016

Performance Analysis of Modified Solar Water Heating System for Climatic Condition of Allahabad, India

Kirti Tewari, Rahul Dev

Open Science Index, Energy and Power Engineering Vol:10, No:1, 2016 publications.waset.org/10003486/pdf

***Abstract*—**Solar water heating is a thermodynamic process of heating water using sunlight with the help of solar water heater. Thus, solar water heater is a device used to harness solar energy. In this paper, a modified solar water heating system (MSWHS) has been proposed over flat plate collector (FPC) and Evacuated tube collector (ETC). The modifications include selection of materials other than glass, and glass wool which are conventionally used for fabricating FPC and ETC. Some modifications in design have also been proposed. Its collector is made of double layer of semi-cylindrical acrylic tubes and fibre reinforced plastic (FRP) insulation base. Water tank is made of double layer of acrylic sheet except base and north wall. FRP is used in base and north wall of the water tank. A concept of equivalent thickness has been utilised for calculating the dimensions of collector plate, acrylic tube and tank.

A thermal model for the proposed design of MSWHS is developed and simulation is carried out on MATLAB for the capacity of 200L MSWHS having collector area of 1.6 m^2, length of acrylic tubes of 2m at an inclination angle 25° which is taken nearly equal to the latitude of the given location. Latitude of Allahabad is 24.45° N. The results show that the maximum temperature of water in tank and tube has been found to be 71.2°C and 73.3°C at 17:00hr and 16:00hr respectively in March for the climatic data of Allahabad.

Theoretical performance analysis has been carried out by varying number of tubes of collector, the tank capacity and climatic data for given months of winter and summer.

***Keywords*—**Acrylic, Fibre reinforced plastic, Solar water Heating, Thermal model, Conventional water heaters.

NOMENCLATURE

T_{FRP} - Temperature of FRP sheet (°C)
T_p - Temperature of absorber plate (°C)
T_{oo} - Temperature of outer surface of outer tube of collector (°C)
T_{oi} - Temperature of inner surface of outer tube (°C)
T_{io} - Temperature of outer surface of inner tube (°C)
T_{Eoo} - Temperature of outer surface of outer layer of east wall (°C)
T_{Eii} - Temperature of inner surface of inner layer of east wall (°C)
T_{Eoi} - Temperature of inner surface of outer layer of east wall (°C)
T_{Eio} - Temperature of outer surface of inner layer of east wall (°C)
T_{sii} - Temperature of inner surface of inner layer of south wall (°C)
T_{wii} - Temperature of inner surface of inner layer of west wall (°C)
T_{topii} - Temperature of inner surface of inner layer of top wall (°C)
T_{No} - Outer surface temperature of north wall (°C)
T_{bi} - Inner surface temperature of bottom wall of tank (°C)
T_{Ni} - Inner surface temperature of north wall (°C)
T_{cw} - Temperature of cold water in tank (°C)
T_{hw} - Temperature of hot water in tube (°C)
T_{hwo} - Initial hot water temperature (°C)
T_{cwo} - Initial cold water temperature (°C)
α_p - Absorptivity of absorber plate
α_{FRP} - Absorptivity of FRP
α_w - Absorptivity of water
α_{acry} - Absorptivity of acrylic tubes
V_a - Velocity of air (m/s)
T_a - Ambient temperature (°C)
N_t - No of tubes
L - Length of tubes (m)
ρ - Density of water (kg/m^3)
τ_w - Transmitivity of water
τ_{acry} - Transmitivity of tubes
A_p - Area of metallic plate (m^2)
A_{iit} - Inside area of inner tube (m^2)
A_{iot} - Outside area of inner tube (m^2)
A_{oit} - Inside area of outer tube (m^2)
A_{oot} - Outside area of outer tube (m^2)
R_{ii} - Inside radius of inner tube (m)
R_{io} - Outside radius of inner tube (m)
R_{oi} - Inside radius of outer tube (m)
R_{oo} - Outside radius of outer tube (m)
A_s - Area of south wall of storage tank (m^2)
A_{top} - Area of top wall of storage tank (m^2)
A_E - Area of east wall of storage tank (m^2)
A_w - Area of west wall of storage tank (m^2)
A_N - Area of north wall of storage tank (m^2)
A_b - Area of bottom wall of storage tank (m^2)
A_{FRP} - Area of insulation of FRP sheet (m^2)
$I_t(t)$ - Solar radiation on collector (W/m^2)
$I_s(t)$ - Solar radiation on south wall of tank (W/m^2)
$I_E(t)$ - Solar radiation on east wall of tank (W/m^2)
$I_w(t)$ - Solar radiation on west wall of tank (W/m^2)
$I_{top}(t)$ - Solar radiation on top wall of tank (W/m^2)
C_w - Specific heat of water (J/kg-k)
t_{FRPi} - Thickness of insulation (m)
t_{FRPt} - Thickness of wall (m)
t_{acry} - Thickness of acrylic wall of tank (m)
K_{FRP} - Thermal conductivity of FRP (W/mK)
K_{acry} - Thermal conductivity of acrylic (W/mK)
M_{tw} - Total mass of water in all tube (Kg)
M_{TW} - Remaining water mass in tank (Kg)
m - Mass flow rate of water (Kg/sec)
h_o - Radiative- convective heat transfer coefficient between outer acrylic tube and ambient as well as between walls of tank and ambient (W/m^2K)
h_i - Radiative heat transfer coefficient between outer surface of inner tube and inner surface of outer tube as well as between south, east, west and top outer surface of inner layer and inner surface of outer layer (W/m^2K)
h_p - Convective heat transfer coefficient between absorber plate and water in tube (W/m^2K)
h_{Tw} - Convective heat transfer coefficient between water in tank and south, east, west and top inner surface of inner layer (W/m^2K)

Kirti Tewari and Rahul Dev are with the Motilal Nehru National Institute of Technology Allahabad, Allahabad 211004 India (phone: +91-8005329107; e-mail: ktkirtitewari@gmail.com, rahuldsurya@yahoo.com).

h_{nw} - Convective heat transfer coefficient between water in tank and inner surface of north wall (W/m^2K)
h_{bw} - Convective heat transfer coefficient between water in tank and inner surface of bottom surface (W/m^2K)

I. Introduction

WATER heating is a very common process which is being used since ancient times for getting hot water. Hot water is required for both industrial processes and household uses. Thus, such technology should be used which can fulfill all the demand of hot water without degrading natural resources and environment. Hence, move toward sustainable development have to be made which can be achieved by judicious use of fuels and by utilising renewable resource such as solar energy. Solar energy is a renewable form of energy and available in abundance which makes it highly appealing source. It can be used for direct conversion into electricity (by photovoltaic conversion) and into thermal energy by solar water heater.

Solar water heater consists of collector and storage tank. Collectors are mainly of three types- FPC, ETC and concentrating solar collectors. FPC is designed to work in low temperature range (ambient temperature-60°C) and medium temperature range (ambient temperature-100°C). Losses are very high in these type of collectors. Convective losses of FPC can be reduced by removing air between absorber and glass cover. The resulting stress will restrict the use of vacuum. Also, maintaining vacuum in FPC is a problem which can be eliminated by ETC. In ETC vacuum is created between glass cover and absorber. Its performance is high only at higher temperature. Thus, both type of collectors has certain limitations and advantages so till now many improvements have been done in this field to eliminate the limitations.

Ammari et al. [1] theoretically as well as experimentally evaluated a tar solar water heater. Here, tar acts as an absorber plate. Runge- Kutta method of fifth order was used to solve three partial differential equations of collector and compared this model with conventional water heaters. Results show that its efficiency is lower in daytime in comparison of conventional heaters but in evening and late afternoon, its performance is found to be better.

Shah et al. [2] presented theoretical study of flow investigation of all glass evacuated tubular collector. The investigations were based on a collector design with horizontal tubes connected to a vertical manifold channel. Three different varying length were modeled with five different inlet mass flow rates at a constant temperature of 333K and found that shortest tube achieved the highest efficiency.

Budihardjo et al. [3] compared experimental and numerically obtained flow rates for natural circulation for evacuated tubes connected with horizontal storage tank. Evacuated tubes used are single-ended water-in-glass and mounted over diffuse reflector. A correlation is developed in terms of aspect ratio of tubes, solar radiations, temperature of tank and inclination of collector. ±5% and ±10% error is found between measured and numerically obtained flow rates for the four tubes which are far from edge in before and after noon respectively.

Zambolin et al. [4] compared standard glazed FPC and direct flow ETC with CPC reflector under same steady state and quasi-dynamic conditions and plotted collected solar energy with solar radiation at constant operating condition (t_m-t_a) and found that FPC is more influenced by this temperature difference. Efficiency curves was obtained by standard EN 12975-2 and conclude that losses in evening and morning is more in FPC and efficiency of ETC is higher than FPC.

Chen et al. [5] calculated the efficiencies of flat plate collectors at different flow rates. Two FPC were tested, one with ETFE foil and other without ETFE foil in Technical University of Denmark. Comparing theoretical and measured values it was observed that start efficiency is higher for without ETFE foil but yearly efficiency of collector with ETFE was higher when fluid collector temperature is 60°C. Volume flow rate was found to have direct relation with incident angle modifier, start efficiency and efficiency and have inverse relation with heat loss coefficient.

Roberts et al. [6] provides analytical expression for instantaneous efficiency of FPC and showed that efficiency get influenced on changing certain parameters for a single glass cover solar hot water heater. In this paper role of absorber plate's emittance and absorptance was studied and found that absorptance should be high for water heaters.

Dev et al. [7] studied the performance of EISS (Evacuated tubular collector integrated solar still) system for composite climatic condition of Delhi and developed thermal model and carried out experiments throughout year (January-December 2008) and obtained higher yield in summer with maximum (annual) thermal efficiency of 30.1%. This system provides distilled as well as hot water.

Taheri et al. [8] presents study of an efficient compact solar water heater. Black coloured sand in the storage tank (1.45 x 0.56 x 0.17m3) of galvanized sheet acts as absorber. Its simulation was carried out using EES software. Experiments with 0.67m2 collector area has been carried out and efficiencies for south-west situation have been found to be greater than 70% due to forced flow operation. CSWH has been found to be economical and have large storage capacity per unit volume. Validation results showed 1.09% and 2.27% as lowest and highest relative errors.

Tse et al. [9] simulated dynamic model on FORTRAN for storage tank, heat exchanger coil, thermosyphon system at night and morning time and carried out experimental validation of thermosyphon solar water heater coupled with a heat exchanger of circular tube rings type. Experimental and simulated results were compared and found to be in good agreement.

In this paper, theoretical performance analysis has been carried out of MSWHS which is a combination of FPC and ETC techniques. On the basis of thermal model, simulation has been carried out on MATLAB and various results have been found for proposed model of MSWHS. Then its various parameters like solar radiation, wind velocity, ambient temperature, capacity of MSWHS and number of tubes have been varied for its performance analysis.

Open Science Index, Energy and Power Engineering Vol:10, No:1, 2016 publications.waset.org/10003486/pdf

Open Science Index, Energy and Power Engineering Vol:10, No:1, 2016 publications.waset.org/10003486/pdf

II. Design of Experimental Setup

Proposed model of MSWHS of 200L capacity consists of collector and storage tank. Collector is made of metallic absorber plate having double layered semi-cylindrical acrylic tubes above it and FRP sheet placed below for insulation. Absorbing area of collector is 1.6m^2 and number of acrylic tubes are 16. Length of tubes is 2m. These tubes are connected with a cuboidal water storage tank (493.6 x 493.6 x 800 mm^3). FRP is used to cover north wall and base of storage tank. East, west, south and top wall of water tank consists of double layer of acrylic sheet. Schematic diagram of proposed MSWHS is shown in Fig. 1 and cross-sectional view of solar collector is shown in Fig. 2. In this paper concept of equivalent thickness has been used to replace glass wool used in conventional collectors with acrylic. Various parameters of MSWHS has been shown in Table I. Thickness of FRP is calculated by (1):

$$t_{FRP} = K_{FRP}\frac{(t_{gw}.K_{m1}) + (t_{m1}.K_{gw})}{K_{gw}.K_{m1}} \quad (1)$$

Equivalent thickness of acrylic tube is calculated by (2)

$$R_{2acry} = R_{1acry}\left[\frac{R_{2g}}{R_{1g}}\right]^{\frac{K_{acry}}{K_g}} \quad (2)$$

Theoretical values of solar radiation, ambient temperature of MSWHS for a day of March is given in Table II and measured values of solar radiation, ambient temperature and wind velocity for summer (June) month is given in Table III.

III. Working Principle

MSWHS is based on thermo-syphon effect. Solar energy falls on acrylic tube which transmits most of it to the water flowing between tubes and metallic plate. Solar radiation which falls on metal plate will also heat the water. Thus, water gets heated by combined effect of both metal plate and heat energy transmitted through tubes. This hot water moves up because of its lower density and cold water from the tank having comparatively higher density will flow down into the tubes. Tank will also contribute into heating of water during sunshine hours as its walls are transparent consisting of acrylic and will reduce heat loss during off sunshine hours because of its design.

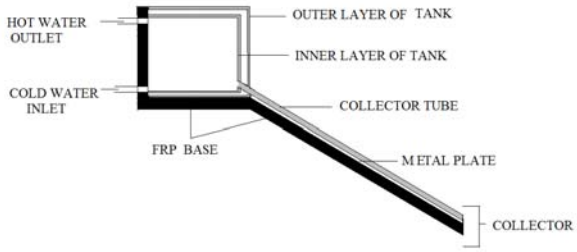


Fig. 1 Schematic diagram of MSWHS



Fig. 2 Cross sectional view of collector

TABLE I
Different Parameters of MSWHS

Specifications	Dimensions	Specifications	Dimensions
α_p	0.95	ρ_w	1000 kg/m^3
α_{FRP}	0.9	L	2m
α_w	0.6	A_P	1.6m^2
α_{acry}	0.05	K_{acry}	0.2 W/m K
τ_{acry}	0.92	R_{ii}	0.01m
τ_w	0.35	R_{i0}	0.0125m
h_i	2.55 W/m^{2}K	R_{oi}	0.022m
N_t	16	R_{oo}	0.025m
$\dot{m}$	0.02 kg/s	$\dot{m}_W$	0.02 kg/s
$V_{1\ tube}$	0.000314 m^3	M_{TW}	194.973 kg
V_T	200 L	K_{FRP}	0.0351 W/mK
M_{tw}	5.026 kg	h_P	200 W/m^{2}K
t_{FRPi}	0.0438m	t_{FRPT}	0.005 m
t_{acryt}	0.003m	A_E	0.243 m^2
A_N	0.394 m^2	A_b	0.394 m^2
A_W	0.243 m^2	Space b/w	0.009 m
A_{top}	0.394 m^2	Tubes	

TABLE II
Hourly Observation of MSWHS of March 15 at Allahabad, India

Time (hr)	$I_G(t)$ (W/m^2)	$I_D(t)$ (W/m^2)	$I_t(t)$ (W/m^2)	$I_E(t)$ (W/m^2)	$I_W(t)$ (W/m^2)	$I_S(t)$ (W/m^2)	$I_{top}(t)$ (W/m^2)	T_a (°C)	Va (m/s)
07:00	190	50	200	200	100	150	150	27.0	1.0
08:00	208	94	420	250	200	330	250	29.0	1.1
09:00	520	176	600	350	320	520	380	32.0	2.0
10:00	600	201	700	540	490	590	420	34.0	2.2
11:00	692	226	800	600	550	650	510	37.0	2.0
12:00	756	229	900	700	600	700	650	39.0	2.0
13:00	736	230	950	900	700	750	720	42.0	2.0
14:00	573	219	820	600	800	600	800	41.0	2.2
15:00	389	163	620	490	600	550	700	40.4	1.9
16:00	332	136	410	210	400	350	600	38.0	1.6
17:00	200	126	250	100	230	150	390	36.0	0.6

TABLE III
HOURLY OBSERVATION OF MSWHS FOR A DAY OF SUMMER (JUNE 15) MONTH AT ALLAHABAD, INDIA

Time (hr)	$I_G(t)$ (W/m^2)	$I_D(t)$ (W/m^2)	$I_t(t)$ (W/m^2)	$I_E(t)$ (W/m^2)	$I_W(t)$ (W/m^2)	$I_S(t)$ (W/m^2)	$I_{top}(t)$ (W/m^2)	T_a (°C)	Va (m/s)
07:00	247	102	400	654	75	200	430	28.0	2.5
08:00	403	165	500	654	108	216	560	31.6	3
09:00	500	192	615	660	144	250	670	33.7	3.5
10:00	668	221	1065	490	205	450	1060	39.3	2.5
11:00	917	232	1195	365	257	460	1150	38.5	3.4
12:00	956	268	1270	204	204	315	1180	36.5	2.5
13:00	633	306	820	133	238	188	1104	33.0	2.8
14:00	300	110	910	168	672	392	929	36.2	2.3
15:00	290	140	850	233	820	380	875	36.2	1.2
16:00	170	101	210	89	144	112	210	34.0	0.7
17:00	122	87	250	69	107	150	153	33.9	0.6

TABLE IV
HOURLY OBSERVATION OF MSWHS FOR A DAY OF WINTER (NOVEMBER 14) MONTH AT ALLAHABAD, INDIA

Time (hr)	$I_G(t)$ (W/m^2)	$I_D(t)$ (W/m^2)	$I_t(t)$ (W/m^2)	$I_E(t)$ (W/m^2)	$I_W(t)$ (W/m^2)	$I_S(t)$ (W/m^2)	$I_{top}(t)$ (W/m^2)	T_a (°C)	Va (m/s)
07:00	200	137	199	200	30	75	173	18.5	0.1
08:00	296	218	382	250	77	80	286	20.5	0.1
09:00	450	298	570	278	85	103	425	22.0	0.2
10:00	600	309	836	310	177	125	625	25.0	0.3
11:00	700	360	940	200	200	193	736	28.2	0.3
12:00	754	419	936	175	200	250	777	29.0	1.2
13:00	605	373	705	110	250	154	620	30.0	1.5
14:00	445	335	610	90	344	100	585	30.5	1.1
15:00	297	209	374	53	205	95	300	30.0	1.0
16:00	100	96	153	29	90	49	100	27.0	0.2
17:00	22	10	25	10	20	15	22	25.5	0.1

IV. THERMAL MODELING

The energy balance for each component of the MSWH has been carried out with the following assumptions,

a. The setup is completely water and vapour leakage proof.
b. The heat capacities of plate, insulations, FRP, Acrylic are negligible.
c. Temperature dependent heat transfer coefficients have been considered.
d. System operates in quasi-steady state regime during the day.
e. The temperature of metal plate and FRP base are considered to be uniform throughout.

A. For Collector

1. For metal plate:

$$\alpha_P\left[\tau_{acry}^2\tau_w I_t(t)\right]A_P = h_p A_P(T_P - T_{hw}) + \frac{K_{FRP}A_{FRP}(T_P - T_{FRP})}{t_{FRPi}} \quad (3)$$

2. For FRP:

$$\frac{K_{FRP}A_{FRP}(T_P - T_{FRP})}{t_{FRPi}} = h_o A_{FRP}(T_{FRP} - T_a) \quad (4)$$

3. For water in Acrylic tube:

$$\alpha_w\tau_{acry}^2 I_t(t)A_{iit}N_t + h_p A_P(T_P - T_{hw}) = M_{tw}C_w\frac{dT_{hw}}{dt} + \dot{m}_w C_w(T_{hw} - T_{cw}) + h_{kacryi}A_{iit}N_t(T_{hw} - T_{io}) \quad (5)$$

4. For outer surface of inner tube:

$$A_{iit}N_t h_{kacryi}(T_{hw} - T_{io}) = h_i A_{iot}N_t(T_{io} - T_{oi}) \quad (6)$$

5. For inner surface of outer tube:

$$h_i A_{oit}N_t(T_{io} - T_{oi}) = h_{kacryo}A_{oot}N_t(T_{oi} - T_{oo}) \quad (7)$$

6. For outer surface of outer tube:

$$h_{kacryo}A_{oot}N_t(T_{oi} - T_{oo}) = A_{oot}N_t h_o(T_{oo} - T_a) \quad (8)$$

Various temperatures will be calculated with the help of above equations and putting the values of T_{io} and T_p in (5), following equation is obtained

$$\frac{dT_{hw}}{dt} + a_1 T_{hw} + b_1 T_{cw} = g_1(t) \quad (9)$$

Open Science Index, Energy and Power Engineering Vol:10, No:1, 2016 publications.waset.org/10003486/pdf

Open Science Index, Energy and Power Engineering Vol:10, No:1, 2016 publications.waset.org/10003486/pdf

B. For Storage Tank

1. For water in storage tank:

$$\begin{aligned}&\alpha_w\left\{I_V(t)A_s+I_H(t)A_{top}\right\}\tau_{acry}^2+\alpha_w\left\{I_E(t)A_E+I_W(t)A_W\right\}\tau_{acry}^2\\&+h_{bw}A_b(T_{bi}-T_{cw})+h_{nw}A_N(T_{Ni}-T_{cw})+\dot{m}_wC_w(T_{hw}-T_{cw})=\\&M_{Tw}C_w\frac{dT_{cw}}{dt}+h_{TW}A_s(T_{cw}-T_{sii})+h_{TW}A_{top}(T_{cw}-T_{topi})+\\&h_{TW}A_E(T_{cw}-T_{Eii})+h_{TW}A_W(T_{cw}-T_{Wii})\end{aligned}\quad(10)$$

2. For east wall (inner surface of inner layer):

$$\alpha_{acry}\left\{I_E(t)A_E\right\}\tau_{acry}+h_{TW}A_E(T_{cw}-T_{Eii})=\frac{K_{acry}A_E(T_{Eii}-T_{Eio})}{t_{acryt}}\quad(11)$$

3. For east wall (outer surface of inner layer):

$$h_{kacry}A_E(T_{Eii}-T_{Eio})=h_iA_E(T_{Eio}-T_{Eoi})\quad(12)$$

4. For east wall (inner surface of outer layer):

$$h_iA_E(T_{Eio}-T_{Eoi})=h_{kacry}A_E(T_{Eoi}-T_{Eoo})\quad(13)$$

5. For east wall (outer surface of outer layer):

$$h_{kacry}A_E(T_{Eoi}-T_{Eoo})=h_oA_E(T_{Eoo}-T_a)\quad(14)$$

6. For north wall (inner surface):

$$\alpha_{FRP}I_V(t)A_N\tau_{acry}^2\tau_w=h_{Nw}A_N(T_{Ni}-T_{cw})+\frac{K_{FRP}A_N(T_{Ni}-T_{No})}{t_{FRPT}}\quad(15)$$

7. For north wall (outer surface):

$$h_{kFRP}A_N(T_{Ni}-T_{No})=h_oA_N(T_{No}-T_a)\quad(16)$$

By putting the values of T_{Eii}, T_{Wii}, T_{Sii}, T_{topii}, T_{bi} & T_{Ni} in (10) and get

$$\frac{dT_{cw}}{dt}+a_2T_{hw}+b_2T_{cw}=g_2(t)\quad(17)$$

Adding (9) and (17) (after multiplying (17) by β) and solving (after multiplying by e^{ct}) further to get,

$$\frac{d}{dt}\left(e^{ct}(T_{hw}+\beta T_{cw})\right)=\left\{g_1(t)+\beta g_2(t)\right\}e^{ct}\quad(18)$$

Further, some assumptions have been made for solving (18),

i. small time interval dt $(0 < t < dt)$
ii. function $f(t)$ are constant, i.e., $f(t)=\overline{f(t)}$ for small interval dt.
iii. a is a constant during the time interval
iv. Initial values of hot water and cold water temperatures have been used to determine value of internal heat transfer coefficients.

From (18) following equations can be obtained: Temperature of cold water in tank:

$$\begin{aligned}T_{cw}=&\frac{1}{\beta^+-\beta^-}\left[\overline{g_1(t)}\left\{\frac{\left(1-e^{-c^+t}\right)}{c^+}-\frac{\left(1-e^{-c^-t}\right)}{c^-}\right\}+\overline{g_2(t)}\right.\\&\left\{\frac{\beta^+\left(1-e^{-c^+t}\right)}{c^+}-\frac{\beta^-\left(1-e^{-c^-t}\right)}{c^-}\right\}+T_{hwo}(e^{-c^+t}-e^{-c^-t})+\\&\left.T_{cwo}(\beta^+e^{-c^+t}-\beta^-e^{-c^-t})\right]\end{aligned}\quad(19)$$

Temperature of hot water in tube:

$$\begin{aligned}T_{hw}=&\frac{1}{\beta^+-\beta^-}\left[\overline{g_1(t)}\left\{\frac{\beta^+\left(1-e^{-c^-t}\right)}{c^-}-\frac{\beta^-\left(1-e^{-c^+t}\right)}{c^+}\right\}+\right.\\&\beta^+\beta^-\overline{g_2(t)}\left\{\frac{\left(1-e^{-c^-t}\right)}{c^-}-\frac{\left(1-e^{-c^+t}\right)}{c^+}\right\}+T_{hwo}(\beta^+e^{-c^-t}-\beta^-e^{-c^+t})+\\&\left.\beta^+\beta^-T_{cwo}(e^{-c^-t}-e^{-c^+t})\right]\end{aligned}\quad(20)$$

IV. Result and Discussion

Hot water temperatures (T_{hw}) and cold water temperatures (T_{cw}) have been computed for all the variations with the help of modeling and plotted against time for 07:00hr to 17:00hr.

Fig. 3 shows the hourly variation of cold water temperatures in water tank with solar radiation and wind velocity from 07:00hr to 17:00hr. Here, measured values of solar radiations for climatic condition of Allahabad in the month of March, July and November have been used to study its performance. Solar radiations on every walls, ambient temperature and wind velocity of MSWHS are shown in Table II for March 15. Measured values of solar radiations, wind velocity and ambient temperature for the month of July15 is shown in Table III and for November 14 in Table IV. From Fig. 3 it is concluded that cold water temperatures obtained for measured solar data of June are higher than that of March. Thus, MSWHS is working better in the summer month (June). Maximum and minimum temperatures of cold water for measured summer (June) solar data has been found to be 72°C and 30°C at 16:00hr and 07:00hr respectively while for solar data of March maximum and minimum temperature of cold water has been found to be 71°C and 30°C at 17:00hr and 07:00hr respectively and for winter (November) maximum and minimum temperatures have been found to be 22°C and 49°C at 17:00hr and 07:00hr respectively.

Fig. 4 shows the hourly variation of hot water temperature in tubes of MSWHS with solar radiations, wind velocity and ambient temperatures. Here hot water temperatures of June are higher than hot water temperatures obtained for the month of March. Minimum temperature has been found to be 35°C and

Open Science Index, Energy and Power Engineering Vol:10, No:1, 2016 publications.waset.org/10003486/pdf

32°C at 07:00hr for June and March respectively and maximum for measured solar data of June is 76.8°C at 15:00hr. Maximum hot water temperature for March is 73.3°C at 16:00hr. In winter (November) minimum temperature of hot water has been obtained in morning at 07:00hr. With increase in solar radiation temperature increases up to 52.76°C at 16:00hr. Thus, in winter month comparatively lower temperatures have been obtained due to lower solar radiation and ambient temperatures.

After varying solar data, number of tubes of collector has been varied and hot water and cold water temperatures have been computed for eleven hours (07:00hr to 17:00hr) for the month of March. Fig. 5 shows hourly variation of hot water temperature with number of tubes. It is clearly shown in figure that hot water temperature of tubes increases with increase in number of tubes. Maximum and minimum temperature for 18 number of tubes has been found to be 76°C at 16:00hr and 35°C at 07:00hr respectively while for 14 number of tubes it is found to be 71°C and 35°C at 16:00hr and 07:00hr respectively.

Fig. 6 shows hourly variation of cold water temperature with number of tubes. As number of tubes increases temperature of cold water in tank also increase because absorbing area of collector and length of tank will increase with number of tubes. 73.6°C and 30°C has been found to be maximum and minimum temperature of cold water in tank at 17:00hr and 07:00hr respectively for MSWHS with 18 number of tubes.

Capacity of MSWHS has also been varied to study its performance by computing hot water and cold water temperatures. Hourly variation of hot water temperature with capacity of MSWHS for the month of March has been shown in Fig. 7. Figure shows inverse relation of capacity of MSWHS with temperature obtained. As capacity increases hot water temperature get reduced. For 300L capacity maximum and minimum temperatures have been found to be 65.4°C and 35°C at 16:00hr and 07:00hr respectively. For 100L capacity maximum and minimum temperatures have been found to be 93.1°C and 35°C at 16:00hr and 07:00hr respectively.

Fig. 8 shows hourly variation of cold water temperature with capacity of MSWHS. Here also, inverse relation between cold water temperature and capacity of MSWHS has been obtained. 91.9°C and 30°C has found to be maximum and minimum temperatures for 100L capacity of MSWHS at 17:00hr and 07:00hr respectively while 62.6°C and 30°C has been found to be maximum and minimum temperatures for 300L capacity of MSWHS at 17:00hr and 07:00hr respectively.

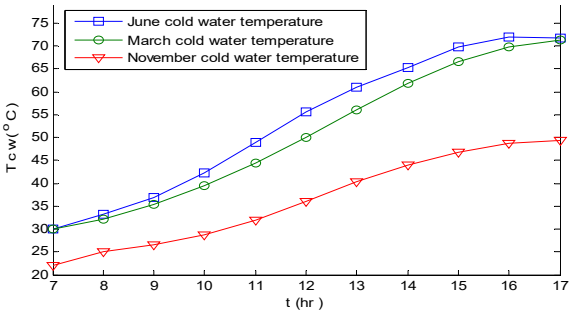


Fig. 3 Hourly variation of cold water temperature with solar data

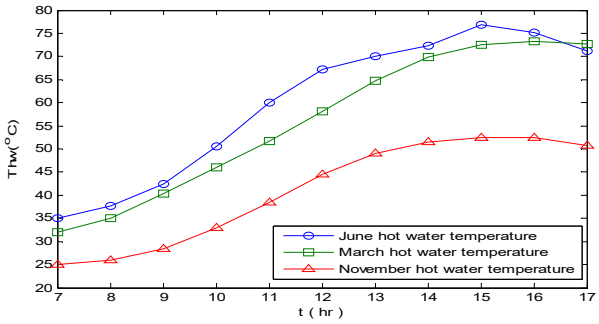


Fig. 4 Hourly variation of hot water temperature with solar data

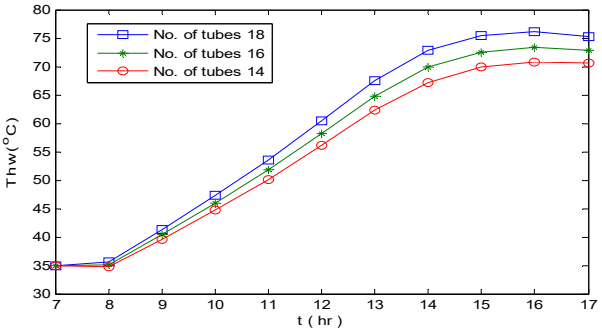


Fig. 5 Hourly variation of hot water temperature with number of tubes

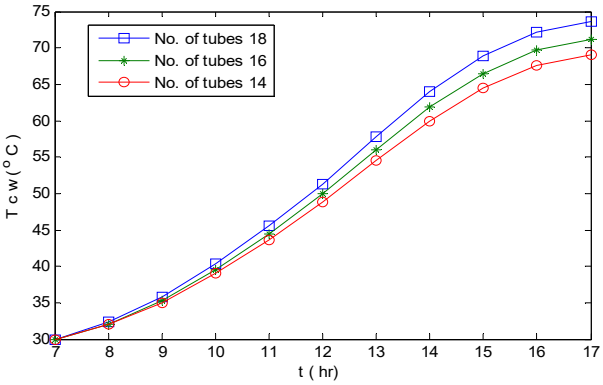


Fig. 6 Hourly variation of cold water temperature with number of tubes

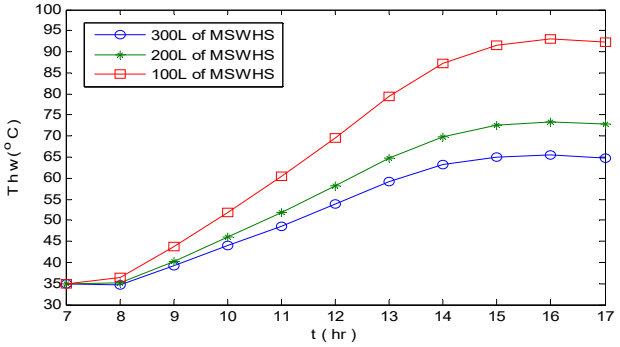


Fig. 7 Hourly variation of hot water temperature with capacity of MSWHS

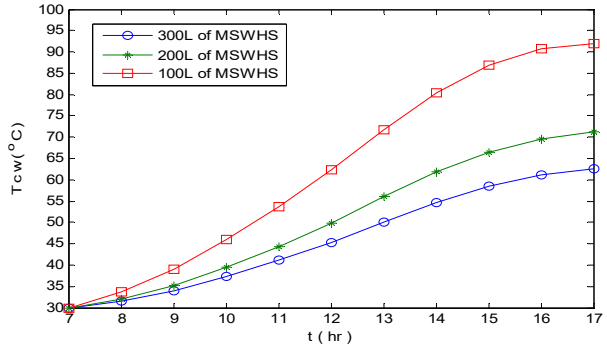


Fig. 8 Hourly variation of cold water temperature with capacity of MSWHS

V. Conclusion

The influence of integration of features of FPC and ETC has been studied in this paper. Due to improvement in material, shape and working principle, the performance of MSWHS has been improved and it is concluded from present study that on increasing the number of tubes of collector or on reducing the capacity of MSWHS, hot water temperatures in tubes of collector and cold water temperatures in tank get increased.

Variation in hot and cold water temperatures are found with change of weather conditions. Maximum variation of hot water temperature between summer and winter month has been found to be 24.3°C at 15:00hr and 21.9°C at17:00hr for cold water temperature.

Maximum variation in hot water temperature of MSWHS with 18 and 14 number of collector tubes has been found to be 5.1°C at 16:00hr. Maximum cold water temperatures obtained are 73.68°C and 69.1°C for 18 and 14 number of tubes at 17:00hr respectively. Thus, increment of 4.6°C has been obtained by increasing 4 number of tubes of collector.

Maximum temperature of hot water temperature has been found to be 93.16°C when capacity of MSWHS is 100L and 65.41°C at 16:00hr for 300L. Thus, maximum of 27.6°C variation has been obtained by varying capacity of MSWHS from 100L to 300L. Maximum cold water temperature has been found to be 91.9°C for 100L capacity and 62.68°C for 300L of MSWHS.

Appendix

Various Intermediate Expressions for Thermal Modeling of MSWHS

$$T_P = \frac{\alpha_P \tau_{acry}^2 \tau_w I_t(t) + h_P T_{hw} + h_{FRP_O} T_a}{U_O}$$

$$T_{oi} = \frac{T_a h_{kacryo_o} + A_1 T_{io} h_i}{U}$$

$$T_{oo} = \frac{h_o T_a + h_{kacryo} T_{oi}}{h_o + h_{kacryo}}$$

$$T_{io} = \frac{T_a V_o + A_2 h_{kacryi} T_{hw}}{V_1}$$

$$T_{Eii} = \frac{\alpha_{acry} I_E(t) \tau_{acry} + h_{TW} T_{cw} + h_c T_a}{U_1}$$

$$T_{bi} = \frac{\alpha_{FRP} I_H(t) \tau_{acry}^2 \tau_w + h_{bw} T_{cw} + T_a h_{kFRP_O}}{U_{2b}}$$

$$T_{topii} = \frac{\alpha_{acry} I_H(t) \tau_{acry} + h_{TW} T_{cw} + h_c T_a}{U_1}$$

$$T_{Eoo} = \frac{h_{kacry} T_{Eoi} + h_o T_a}{h_{kacry} + h_o}$$

$$T_{Eio} = \frac{T_{Eii} h_A + T_a h_B}{h_A + h_B}$$

$$T_{Ni} = \frac{\alpha_{FRP} I_V(t) \tau_{acry}^2 \tau_w + h_{Nw} T_{cw} + T_a h_{kFRP_O}}{U_{2N}}$$

$$b_1 + \beta b_2 = \beta c, \quad a_1 + \beta a_2 = c$$

$$\beta = \frac{-(a_1 - b_2) \pm \sqrt{(a_1 - b_2)^2 - 4a_2(-b_1)}}{2a_2}$$

$$U_O = h_P + \frac{K_{FRP}}{t_{FRP}} - \frac{K_{FRP}^2}{t_{FRP}(K_{FRP} + h_o t_{FRP})}$$

$$V_o = \frac{h_{kacryo-o} h_i}{U}, \quad A_2 = \frac{A_{iit}}{A_{oit}}$$

$$U = \frac{h_{kacryo} h_o + A_1(h_o + h_{kacryo}) h_i}{h_o + h_{kacryo}}$$

$$V_1 = h_i + h_{kacryi} A_2 - \frac{A_1 h_i^2}{U}$$

$$h_{kacry} = \frac{K_{acry}}{t_{acryt}}$$

$$a_1 = \frac{\dot{m}_w C_w + A_{iit} N_t h_{kacryi} + h_p A_p}{M_{tw} C_w} - \frac{h_p^2 A_p}{V_o M_{tw} C_w} - \frac{A_{iit} N_t h_{kacryi}^2}{V_1 M_{tw} C_w}$$

$$b_1 = \left(- \frac{\dot{m}_w}{M_{tw}} \right)$$

$$b_2 = \left(\frac{h_{bw} A_b + h_{Nw} A_N}{M_{Tw} C_w} \right) + h_{TW}^2 \left(\frac{-A_S - A_E - A_W - A_{top}}{M_{Tw} C_w U_1} \right) + \frac{h_{TW}}{M_{Tw} C_w} \left(A_S + A_E + A_W + A_{top} \right)$$

$$+ \frac{1}{M_{TW} C_w} \left(- \frac{h_{bw}^2 A_b}{U_{2b}} - \frac{h_{Nw}^2 A_N}{U_{2N}} \right) + \frac{\dot{m}_w C_w}{M_{Tw} C_w}$$

$$g_1(t) = \frac{\alpha_w \tau_{acry}^2 I_t(t) A_{iit} N_t}{M_{tw} C_w} + \frac{h_p A_p \alpha_p \tau_{acry}^2 \tau_w I_t(t)}{U_o M_{tw} C_w} + \frac{h_p A_p h_{FRP_O} T_a}{U_o M_{tw} c_w} + \frac{A_{iit} N_t h_{kacryi} V_o T_a}{V_1 M_{tw} C_w}$$

Open Science Index, Energy and Power Engineering Vol:10, No:1, 2016 publications.waset.org/10003486/pdf

$$g_2(t)=\frac{\alpha_w\tau_{acry}^2}{M_{Tw}C_w}\left(I_V(t)A_S+I_H(t)A_{top}+I_E(t)A_E+I_W(t)A_W\right)+\frac{\tau_{acry}^2\alpha_{FRP}\tau_w}{M_{Tw}C_w}\left(\frac{I_H(t)h_{bw}A_b}{U_{2b}}+\frac{I_V(t)h_{Nw}A_N}{U_{2N}}\right)$$

$$+\frac{h_{TW}\tau_{acry}\alpha_{acry}}{M_{Tw}C_wU_1}\left(I_V(t)A_S+I_H(t)A_{top}+I_E(t)A_E+I_W(t)A_W\right)$$

$$+\frac{T_ah_{kFRP_O}}{M_{Tw}C_w}\left(\frac{h_{bw}A_b}{U_{2b}}+\frac{h_{Nw}A_N}{U_{2N}}\right)+\frac{h_{TW}h_cT_a}{M_{Tw}C_wU_1}\left(A_S+A_E+A_W+A_{top}\right)$$

$$h_{okacry}=h_oh_{kacry}$$

$$h_{ikacry}=h_ih_{kacry}$$

$$h_A=h_{kacry}h_{ikacry}+h_{kacry}h_{io}+h_{kacry}h_{okacry}$$

$$h_B=h_ih_{okacry}$$

$$h_{io}=h_ih_o$$

$$U_1=\frac{h_{TW}h_A+h_{TW}h_B+h_Bh_{kacry}}{h_A+h_B}$$

$$h_c=\left(\frac{h_{kacry}h_B}{h_A+h_B}\right)$$

$$h_{kFRP_O}=\frac{h_{kFRP}h_o}{h_o+h_{kFRP}}$$

$$h_{kFRP}=\frac{K_{FRP}}{t_{FRPt}}$$

$$U_{2N}=\frac{h_{Nw}h_o+h_{Nw}h_{kFRP}+h_oh_{kFRP}}{h_o+h_{kFRP}}$$

$$U_{2b}=\frac{h_{bw}h_o+h_{bw}h_{kFRP}+h_oh_{kFRP}}{h_o+h_{kFRP}}$$

$$a_2=\left(-\frac{\dot{m}_w}{M_{Tw}}\right)$$

$$A_1=\frac{A_{oit}}{A_{oot}}$$

$$h_{kacryo_o}=\frac{h_{kacryo}h_o}{h_o+h_{kacryo}}$$

$$h_{FRP_O}=\frac{K_{FRP}h_o}{K_{FRP}+h_ot_{FRP}}$$

$$T_{Sii}=\frac{\alpha_{acry}I_V(t)\tau_{acry}+h_{TW}T_{cw}+h_cT_a}{U_1}$$

$$T_{Wii}=\frac{\alpha_{acry}I_w(t)\tau_{acry}+h_{TW}T_{cw}+h_cT_a}{U_1}$$

$$T_{No}=\frac{T_{Ni}h_{kFRP}+T_ah_o}{h_{kFRP}+h_o}$$

REFERENCES

[1] H.D. Ammari, Y.L. Nimir, "Experimental and theoretical evaluation of the performance of a tar solar water heater", Department of Mechanical Engineering, Faculty of Engineering, Mu'tah University, Karak, Jordan, Energy Conversion and Management, vol. 44, pp. 3037–3055, Feb. 2003.

[2] L.J. Shah, S. Furbo, "Vertical evacuated tubular-collectors utilizing solar radiation from all directions", Applied Energy vol. 78, pp. 371-395, 2004.

[3] Indira Budihardjo, Graham L. Morrison, Masud Behnia, "Natural circulation flow through water-in-glass evacuated tube solar collectors", School of mechanical Engineering, University of New South Wales, NSW 2032, Austrailia, vol. 81, pp. 1460-1472, April 2007.

[4] E. Zambolin, D. Del Col, "Experimental analysis of thermal performance of flat plate and evacuated tube solar collectors in stationary standard and daily conditions", Dipartimento di Fisica Tecnica, Universita` degli Studi di Padova, Via Venezia 1, 35131 Padova, Italy, Solar Energy vol. 84, pp.1382–1396, June 2010.

[5] Ziqian Chen, a Simon Furbo, Bengt Perers, Jianhua Fan, Elsa Andersen, "Efficiencies of flat plate solar collectors at different flow rates", Department of Civil Engineering, Technical University of Denmark, Kgs. Lyngby, Denmark, Energy Procedia, vol. 30, pp. 65 – 72. 2102.

[6] D.E. Roberts, A. Forbes, "An analytical expression for the instantaneous efficiency of a flat plate solar water heater and the influence of absorber plate absorptance and emittance,",Council for Scientific and Industrial Research, National Laser Centre, Building 46, P.O. Box 395, Pretoria 0001, Gauteng, South Africa, School of Physics, University of KwaZulu-Natal, Private Bag X54001, Durban 4000, South Africa, Solar Energy, vol. 86, pp. 1416–1427, March 2012.

[7] Rahul Dev, G. N Tiwari, "Annual performance of evacuated tubular collector integrated solar still", Centre for Energy Studies, IIT Delhi, Haus Khas, New Delhi110016, India, vol 41, pp. 204-223, February 2012.

[8] Y. Taheri, Behrooz M. Ziapour, K. Alimardani, "Study of an efficient compact solar water heater", Department of Mechanical Engineering University of Mohaghegh Ardabili, Ardabil,Iran, Energy Conversion and Management, vol. 70, pp.187–193, April 2013.

[9] Ka-Kui Tse, Tin-Tai Chow, "Dynamic model and experimental validation of and indirect thermosyphon solar water heater coupled with a parallel circular tube rings type heat exchange coil", Building Energy and Environmental Technology Research Unit, Division of Building Science and Technology, City University of Hong Kong, Kowloon, Hong Kong, China, Solar Energy, vol.114, pp.114–133, Feb. 2015.

Open Science Index, Energy and Power Engineering Vol:10, No:1, 2016 publications.waset.org/10003486/pdf